A Meshed Hybrid Microgrid Configuration with Unified Power Quality Conditioner

Kumar, Devendra; Hrishikesan, V. M.; Deka, Anup Kumar; Das, Dwijasish; Kumar, Chandan; Mishra, Mahesh K.

DOI
10.1109/JESTPE.2025.3536859

Publication date
2025

Document Version
Final published version

Published in
IEEE Journal of Emerging and Selected Topics in Power Electronics

A Meshed Hybrid Microgrid Configuration With Unified Power Quality Conditioner

Devendra Kumar, *Student Member, IEEE*, V. M. Hrishikesan, Anup Kumar Deka, Dwijasish Das, *Member, IEEE*, Chandan Kumar, *Senior Member, IEEE*, and Mahesh K. Mishra, *Senior Member, IEEE*

***Abstract*— The distribution grid is under major transformation due to the increasing dependency on renewable energy resources (RESs) and electric vehicle (EV) charging stations. For accommodating such sources and loads in an existing ac distribution system without violating the voltage and current quality limits, various strategies, such as modifying the control methodologies and structural reconfiguration of the grids, are identified as suitable options. The power electronic converters play a significant role in integrating these features to the distribution grid. A unified power quality conditioner (UPQC) is a preferred choice to control the quality of both currents and voltages. In this article, the operation of a meshed hybrid microgrid is realized using UPQC. The dc link of UPQC is used to form a low voltage dc (LVdc) line. This LVdc line is connected parallel to the low voltage ac (LVac) lines. The loads and distribution generation units are integrated to ac and dc lines using power electronic converters. The improved performance during adverse operating conditions shows the superior reliability of the proposed system. In addition, the analysis verifies the enhanced capability of the proposed system in accommodating new dc loads to the existing system. Both simulation and experimental results are demonstrated to evaluate the performance of the proposed system.**

***Index Terms*— Battery energy storage systems (BESSs), meshed hybrid microgrid, power quality, unified power quality conditioner (UPQC).**

NOMENCLATURE

PCC	Point of common coupling.
RESs	Renewable energy sources.
BESS	Battery energy storage system.
PV	Solar photovoltaic system.
EV	Electric vehicle.
LVac	Low voltage ac.
LVdc	Low voltage dc.
i	Bus number, where $i \in \{1, 2, \ldots, n-1, n\}$.
V_{dc}	DC link voltage of unified power quality conditioner (UPQC).
V_t	LVac grid terminal voltage.
V_f	Voltage injected by UPQC series converter.
V_l	LVac PCC voltage.
P_{net}	Net dc load power in LVdc grid.
$S_{r\text{EV}-i}$	EV dc–ac converter rating.
$P_{\text{EV}-i}$	EV load power.
$S_{r\text{PV}-i}$	PV dc–ac converter rating.
$P_{\text{PV}-i}$	PV active power.
S_{r-m}	Faulty PV or EV dc–ac converter rating.
S_{rC-i}	Healthy PV or EV dc–ac converter rating.
P_{C-i}	Healthy PV or EV dc–ac converter active power.
$S_{t-\text{rat}}$	Total rating of PV and EV dc–ac converter.
P_D	UPQC shunt converter active power.
P_{lv}	LVac load active power measured at PCC.
$P_{\text{dcl}-i}$	DC load power.

Received 3 August 2024; revised 21 November 2024 and 9 January 2025; accepted 14 January 2025. Date of publication 29 January 2025; date of current version 18 April 2025. This work was supported in part by the Science and Engineering Research Board (SERB), Department of Science and Technology, India, under Grant CRG/2022/001685; and in part by the IIT Guwahati Technology Innovation and Development Foundation (TIDF) under Grant TIH/TD/0407. Recommended for publication by Associate Editor Gab-Su Seo. *(Corresponding author: Devendra Kumar.)*

Devendra Kumar and Chandan Kumar are with the Electronics and Electrical Engineering Department, Indian Institute of Technology Guwahati, Guwahati, Assam 781039, India (e-mail: devendrakmrnit@gmail.com; chandank@iitg.ac.in).

V. M. Hrishikesan is with Siemens Gamesa Renewable Energy, 2800 Kongens Lyngby, Denmark (e-mail: hrishieee@gmail.com).

Anup Kumar Deka is with Wright Electric Inc., Malta, NY 12020 USA (e-mail: anupdeka02@gmail.com).

Dwijasish Das is with the Department of Electrical Sustainable Energy, Delft University of Technology (TU Delft), 2628 CD Delft, The Netherlands (e-mail: d.das-1@tudelft.nl).

Mahesh K. Mishra is with the Department of Electrical Engineering, Indian Institute of Technology Madras, Chennai 600036, India (e-mail: mahesh@ee.iitm.ac.in).

Color versions of one or more figures in this article are available at https://doi.org/10.1109/JESTPE.2025.3536859.

Digital Object Identifier 10.1109/JESTPE.2025.3536859

I. INTRODUCTION

IN CONVENTIONAL ac microgrid, the integration of distributed generation (DG) units, EVs, and BESSs, is a challenging task. Various power conversion stages are necessary for safe and reliable integration of these sources and loads to the ac microgrid [1], [2], [3]. Conventionally, the PV-based DGs and BESSs are connected to the ac grid with the help of dc–ac and dc–dc converters [4]. Various type of loads such as EVs, office, and household appliances internally require LVdc and need different types of power conversion stages to connect with ac grid. The power electronic devices introduce various concerns in the distribution grid, such as current and voltage harmonics [1]. Voltage rise is another issue that frequently occurs due to the reverse power flow in grids with high renewable penetration [5]. The load and generation hosting capacity of an existing ac system is limited by the voltage limit violations and overloading of existing components [6], [7]. Therefore, improved methods are necessary to accommodate the extra loads and sources. The architectural modification of the conventional microgrid structure is a promising solution for addressing these issues. Hybrid ac/dc microgrids offer higher flexibility for the integration of DGs, EVs, and

other loads, as they offer both ac and dc voltage levels for interconnection [8]. Recently, meshed hybrid microgrids are gaining prominence with improved reliability for power supply [9], [10]. It has been shown that the interlinking power electronic converters are necessary to form meshed hybrid configurations.

In [11] and [12], the application of a PV system for power quality improvement has been proposed. However, such PV system fails to adequately maintain the LVac grid voltage during the voltage disturbances (such as grid voltage sag, swell, unbalance) due to environment dependency of PV active power. Also, large support of reactive power by PV converter may result in curtailment of the active power of PV source [13], [14].

Conventionally, the distribution static compensator (D-STATCOM) is used to provide the harmonic and reactive power support to the distribution system [15]. The dynamic voltage restorer (DVR) is used for protecting the distribution system from grid voltage variations [16]. The UPQC combines the services of both DVR and D-STATCOM, and they are employed for providing features such as voltage support to voltage sensitive load and current harmonic compensation, respectively. Recently, capabilities of the UPQC for PV integration at dc link is explored [17], [18], [19]. The PV at the UPQC dc link supports active and reactive power to the ac grid. Moreover, due to the lack of a BESS, the UPQC shunt converter cannot achieve bidirectional active power flow. The open-UPQC configuration uses separate dc link capacitors [13]. In this configuration, the PV source is connected to the dc link of shunt compensator. This protects the voltage-sensitive loads and eliminates various load unbalance conditions in a distribution system. In [14] and [20], the UPQC configuration with the integration of BESS and PV systems to the common dc link is analyzed under different operating scenarios. The configuration presented in [20] and [21] shows the performance of UPQC-based PV–BESS system in maintaining the power quality standards during PV power variations and grid voltage sag/swell.

The PV- and BESS-based UPQC systems have the potential to create the dc distribution system parallel to the existing ac distribution system. Such configuration can accommodate more loads and provides power routing between LVac and LVdc buses. This article proposes a meshed hybrid microgrid configuration using UPQC, PV, EV, and BESS. An analysis has been done to show that the proposed UPQC configuration accommodates more loads and RESs in comparison to the existing system.

In comparison with traditional UPQC-based hybrid microgrids, the meshed hybrid microgrids with UPQC present several distinct advantages.

1) The meshed hybrid microgrids with UPQC maintain a balanced and sinusoidal voltage at LVac PCC. It also mitigates harmonic and reactive currents drawn by LVac load currents, enabling the grid to provide balanced sinusoidal currents at unity power factor.
2) UPQC facilitates centralized control of reactive power within the LVac grid. The LVac grid voltage is maintained within grid code limits either with peak PV power injection or EV loading.
3) It ensures reliable operation in the event of a failure in the dc–ac converter of the PV/EV DG system.
4) Increases the utilization of PV/EV dc–ac converter.

This articleis organized as follows. The system configuration is described in Section II. The proposed power management algorithm is explained in Section III. Various power converter control strategies are explained in Section IV. Section V contains the performance analysis focusing on the loading capacity of the distribution system. The simulation and experimental results are provided in Sections VI and VII, respectively. Section VIII provides conclusion to this article.

II. System Configuration

A conventional LVac microgrid configuration with UPQC is shown in Fig. 1(a). In this configuration, the BESS is connected at UPQC dc link using a dc–dc converter. An LVac grid is considered with a number of PV-based DG sources, and EV charging stations are connected at different LVdc buses.

The configuration of the meshed hybrid microgrid is shown in Fig. 1(b). The dc link of UPQC is extended parallel to the LVac line. The BESS connection remains same as shown in Fig. 1(a). The PV-based DGs are connected to the LVdc line at their original locations through the dc–dc converters. Similarly, the EV and dc loads are connected at their locations through the dc–dc converters. The EV and PV dc–ac converters are interlinked between the ac and dc distribution lines at their original location. The presence of dc–ac converters at various locations enable to form multiple meshed loops in the distribution grid.

The BESS maintains the dc link voltage of the UPQC while supplying the power losses in the UPQC. Moreover, the BESS exchanges active power with the LVdc grid to ensure a constant dc link voltage. For realizing it, the BESS also supplies losses in the LVdc line.

The proposed meshed hybrid network consists of two parallel grids to exchange active power between the LVac and LVdc grids. Moreover, the UPQC allows bidirectional active power flow and control of reactive power in the meshed hybrid microgrid. The UPQC in support of reactive power ensures that DG dc–ac converters are utilized for active power exchange. The DG converter can exchange active power between LVac and LVdc grids to maintain the far-end LVac bus voltage within grid code limits. Moreover, the performance of PV and EVs connected at the LVdc grid remains unaffected during faults or maintenance of any DG converter.

In this article, the UPQC performs multiple roles. It maintains the LVac PCC load voltage within grid code limits during any voltage disturbance. It also maintains grid currents balance, sinusoidal and at unity power factor by supplying the reactive and harmonic components of load current. Also, the energy storage at the dc link of UPQC allows exchange of active power with the LVac grid based on requirements. Furthermore, a meshed hybrid microgrid with UPQC provides multiple paths for power flow between LVac and LVdc grids. The UPQC manages the active power flow between the LVac and LVdc grids during peak PV generation, high-EV loading, and DG converter failures. Since the UPQC provides the reactive power demands of the LVac loads, reactive power from the DG converters connected between the LVac and LVdc

buses can be set to 0 increasing the utilization of the DG converters.

III. Proposed Power Management Algorithm

The power management algorithm is used to serve the following objectives: 1) maintain grid currents balanced and sinusoidal at unity power factor; 2) active power routing between LVac and LVdc line during peak load/generation scenarios; 3) maintain LVac PCC voltage magnitude at nominal value; and 4) control active power exchange between LVac and LVdc lines during dc–ac converter failure conditions. The UPQC series converter maintains the LVac PCC voltage magnitude despite the disturbance in grid voltage. Moreover, the shunt converter of UPQC allows LVac loads to draw the balanced and sinusoidal component of current at the unity power factor from the grid. This converter also provides harmonics, unbalanced, and reactive components of load current. Furthermore, dc–ac converters connected between LVac and LVdc grids can exchange the active power.

The proposed power management algorithm flowchart is shown in Fig. 2. The operation of the system shown in Fig. 1(b), can be classified into two modes: 1) normal operation in which all the converters are working based on their ratings, and 2) converter fault operation where some dc–ac converters became faulty during the operation. The active power reference for PV/EV dc–ac converters and UPQC shunt converter are calculated in each mode of operation. Net load active power (P_{net}) on the LVdc line is obtained as follows:

$$P_{\text{net}} = \sum_{i=1}^{n} (P_{\text{EV}-i} + P_{\text{dcl}-i} - P_{\text{PV}-i}) \tag{1}$$

where $P_{\text{EV}-i}$, $P_{\text{PV}-i}$, and $P_{\text{dcl}-i}$ are the ith EV, PV, and dc load power, respectively. The each mode of operation are explained in Section III.

A. Normal Operation

In this mode of operation, all the dc—ac converters are working in normal condition and a satisfactory operation is observed. Total power rating of EV and PV dc—ac converters ($S_{t-\text{rat}}$) is given as follows:

$$S_{t-\text{rat}} = \sum_{i=1}^{n} (S_{rEV-i} + S_{rPV-i}) \tag{2}$$

where S_{rEV-i} and S_{rPV-i} are EV and PV dc—ac converters rating, respectively. The dc—ac converters of PV and EV share active power with the grids based on the P_{net} obtained from (1). Furthermore, UPQC supplies reactive power requirements of LVac loads so that the grid current is balanced and sinusoidal at the unity power factor. Therefore, the reactive power reference of PV/EV dc—ac converters is set to zero in the proposed work. However, this converter can support reactive power in case there is a specific requirement. However, it will lead to a reduction in active power from the converter.

If P_{net} is positive, then the overall power demand in the dc grid exceeds the available generation capacity. If P_{net} is negative then the generation capacity within the dc grid from sources like solar PV, EV is greater than the power demand. When P_{net} is 0, it signifies a perfect balance between generation and consumption within the dc grid.

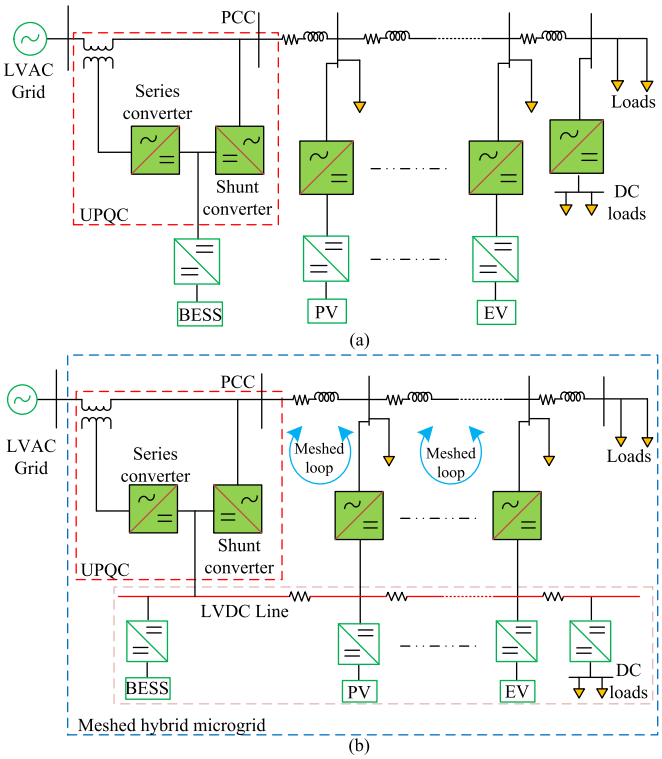

Fig. 1. System configuration. (a) UPQC connected conventional ac microgrid [20]. (b) Proposed UPQC enabled meshed hybrid microgrid.

$S_{t-\text{rat}}$ obtained from (2) is greater than or equal to $|P_{\text{net}}|$, then the active power for ith dc—ac converter of PV and EV are given as follows:

$$P^*_{\text{PV}-i} = \frac{P_{\text{net}} \times S_{rPV-i}}{S_{t-\text{rat}}}$$
$$P^*_{\text{EV}-i} = \frac{P_{\text{net}} \times S_{rEV-i}}{S_{t-\text{rat}}} \tag{3}$$

where $P^*_{\text{PV}-i}$, and $P^*_{\text{EV}-i}$ are the active power reference of PV and EV dc—ac converters, respectively.

If $S_{t-\text{rat}} < |P_{\text{net}}|$, then ith dc—ac converter of PV and EV exchanges maximum active power from the grid and these are given as follows:

$$P^*_{\text{PV}-i} = S_{rPV-i}$$
$$P^*_{\text{EV}-i} = S_{rEV-i}. \tag{4}$$

The shunt converter of UPQC exchanges the balance active power from the grid to meet the excess power requirement at the LVdc line. Therefore, active power reference for the UPQC shunt converter (P^*_D) is given by

$$P^*_D = P_{\text{net}} - S_{t-\text{rat}}. \tag{5}$$

In this condition, excess power due to high loading on LVdc line is routed from LVac to LVdc line via UPQC shunt converter. Therefore, LVac line voltage profile improves during generation or peak load.

B. Converter Fault Operation

In this mode of operation, the meshed hybrid microgrid is operated with a faulty PV/EV dc—ac converter. Then the active power is shared between ac and dc grids using healthy

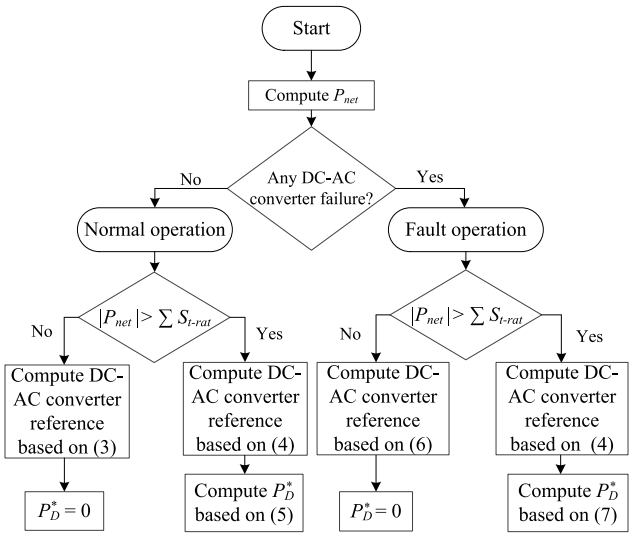

Fig. 2. Flowchart for power management.

PV/EV dc—ac converters. Therefore, the ith PV/EV converter active power is given by

$$P_{C-i}^* = \frac{P_{\text{net}} \times S_{rC-i}}{S_{t-\text{rat}} - S_{r-m}}, \quad \text{if } |P_{\text{net}}| \le S_{t-\text{rat}} - S_{r-m} \tag{6}$$

where P_{C-i}^* is the PV/EV dc—ac converter active power reference, S_{rC-i} is apparent power rating of PV/EV dc—ac converter, and S_{r-m} is the apparent power rating of the faulty dc—ac converter of PV/EV at mth bus. The faulty PV/EV converters are disconnected from the operation. The healthy PV/EV dc—ac converters share the active power based on their power rating.

If the total power rating of the healthy dc—ac converter is less than $|P_{\text{net}}|$, then the active power reference for UPQC shunt converter using (1) and (2), and S_{r-m} is given by

$$P_D^* = P_{\text{net}} - (S_{t-\text{rat}} - S_{r-m}). \tag{7}$$

Therefore, the proposed meshed hybrid microgrid configuration with UPQC maintains the continuity of active power exchange after the removal of the faulty dc—ac converter. Moreover, this capability is not possible in the conventional configuration of microgrid as shown in Fig. 1(a). In the proposed configuration, individual PV/EV dc—ac converter works as both source and load.

IV. Control of Power Converters

Several power converters are configured in the meshed hybrid microgrid. The control diagram of the proposed configuration is shown in Fig. 3. The explanation of UPQC converters, BESS dc–dc converter, PV, and EV dc—ac converter are given in this section.

A. UPQC Converters

There may be several nonlinear loads connected at the LVac grid. The control algorithm calculates the harmonic current components as well as reactive and unbalance currents, and these LVac load current components are supplied by the UPQC shunt converter. Also, any harmonics and disturbance in source voltage are compensated by the series converter of UPQC. The UPQC shunt and series converters control strategy are explained as follows.

1) UPQC Shunt Converter: The primary control objective of the UPQC shunt converter is to supply the reactive and harmonic power of LVac load. The active power exchange is also facilitated through this converter as a secondary requirement. This converter works as a current-controlled device. An instantaneous symmetrical component theory (ISCT) [22] is used for power sharing at the LVac and LVdc grids. The reference currents (i_{daa}^*, i_{dab}^*, and i_{dac}^*) to share the active power by the UPQC shunt converter are given as follows:

$$\begin{aligned} i_{daa}^* &= \frac{v_{la1}^+}{\left(v_{la1}^+\right)^2 + \left(v_{lb1}^+\right)^2 + \left(v_{lc1}^+\right)^2} P_D^* \\ i_{dab}^* &= \frac{v_{lb1}^+}{\left(v_{la1}^+\right)^2 + \left(v_{lb1}^+\right)^2 + \left(v_{lc1}^+\right)^2} P_D^* \\ i_{dac}^* &= \frac{v_{lc1}^+}{\left(v_{la1}^+\right)^2 + \left(v_{lb1}^+\right)^2 + \left(v_{lc1}^+\right)^2} P_D^* \end{aligned} \tag{8}$$

where v_{la1}^+, v_{lb1}^+, and v_{lc1}^+ are the fundamental components of positive sequence voltage of three phases at LVac PCC, and P_D^* is the dc power reference of UPQC shunt converter. P_D^* in (8) is derived from (5) and (7) during normal and fault operations, respectively.

The UPQC shunt converter reference currents (i_{dha}^*, i_{dhb}^*, and i_{dhc}^*) to share the reactive and harmonic component of LVac load currents are given as follows:

$$\begin{aligned} i_{dha}^* &= i_{\text{lv}a} - \frac{v_{la1}^+}{\left(v_{la1}^+\right)^2 + \left(v_{lb1}^+\right)^2 + \left(v_{lc1}^+\right)^2} P_{\text{lv}} \\ i_{dhb}^* &= i_{\text{lv}b} - \frac{v_{lb1}^+}{\left(v_{la1}^+\right)^2 + \left(v_{lb1}^+\right)^2 + \left(v_{lc1}^+\right)^2} P_{\text{lv}} \\ i_{dhc}^* &= i_{\text{lv}c} - \frac{v_{lc1}^+}{\left(v_{la1}^+\right)^2 + \left(v_{lb1}^+\right)^2 + \left(v_{lc1}^+\right)^2} P_{\text{lv}} \end{aligned} \tag{9}$$

where P_{lv} is the average load power measured at PCC. $i_{\text{lv}a}$, $i_{\text{lv}b}$, and $i_{\text{lv}c}$ are instantaneous LVac load currents measured at PCC.

The UPQC shunt converter reference currents ($i_{\text{sh}a}^*$, $i_{\text{sh}b}^*$, and $i_{\text{sh}c}^*$) using (8) and (9) are given as follows:

$$\begin{aligned} i_{\text{sh}a}^* &= i_{\text{lv}a} - \frac{v_{la1}^+}{\left(v_{la1}^+\right)^2 + \left(v_{lb1}^+\right)^2 + \left(v_{lc1}^+\right)^2} \left(P_{\text{lv}} - P_D^*\right) \\ i_{\text{sh}b}^* &= i_{\text{lv}b} - \frac{v_{lb1}^+}{\left(v_{la1}^+\right)^2 + \left(v_{lb1}^+\right)^2 + \left(v_{lc1}^+\right)^2} \left(P_{\text{lv}} - P_D^*\right) \\ i_{\text{sh}c}^* &= i_{\text{lv}c} - \frac{v_{lc1}^+}{\left(v_{la1}^+\right)^2 + \left(v_{lb1}^+\right)^2 + \left(v_{lc1}^+\right)^2} \left(P_{\text{lv}} - P_D^*\right). \end{aligned} \tag{10}$$

The hysteresis-based current controller is used to control the UPQC shunt converter [22]. This controller generates the pulses by comparing the actual currents of the UPQC shunt converter with the reference currents obtained from (10) of the UPQC shunt converter.

2) UPQC Series Converter: The series converter is used to maintain the PCC voltage balanced and sinusoidal at nominal value during the grid voltage disturbances like sag/swell, unbalanced, and harmonics. This converter maintains the PCC voltage for grid voltage sag/swell by exchanging the active power from the dc link [23]. The series converter absorbs

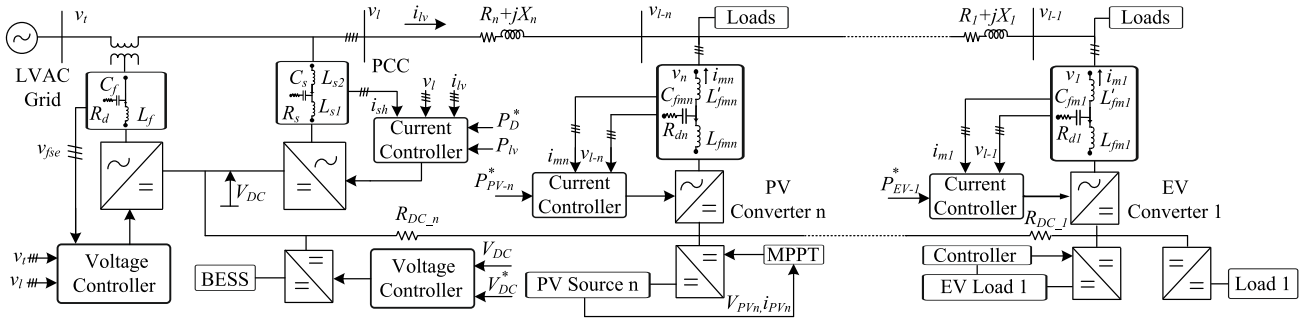

Fig. 3. Overall control diagram of the meshed hybrid microgrid.

the active power during grid voltage sag conditions from dc link and supplies the active power to the dc link during grid voltage swell conditions. Moreover, the active power exchange is directly controlled by BESS to maintain dc link voltage at the desired level. The appropriate reference three-phase voltages are generated for the series converter to maintain the PCC voltage at the desired level. The explanation for the voltage reference of the series converter is given as follows.

The LVac grid terminal voltage (v_t) is expressed in (11) as the sum of fundamental positive sequence components and harmonic components of voltage. The grid terminal voltage is written as follows:

$$v_t = v_{t_1} + v_{t_{\text{rest}}} \tag{11}$$

where v_{t_1} is the fundamental positive sequence component of LVac grid terminal voltage, and its harmonic voltage component is $v_{t_{\text{rest}}}$. The fundamental positive sequence component of series converter voltage is v_{f_1}. The balanced three-phase voltages are maintained at PCC by the UPQC series converter. Hence, the reference voltage ($\mathbf{V_l}^*$) at PCC with the help of Kirchhoff's voltage law (KVL) is expressed as follows:

$$\mathbf{V_l^*} = \mathbf{V_{t_1}} + \mathbf{V_{f_1}}. \tag{12}$$

The fundamental positive sequence component of terminal voltage is expressed as $\mathbf{V_{t_1}} = V_{t_1}\angle\delta_{t_1}$. Assume that the reference voltage is maintained at the PCC, which is expressed as $\mathbf{V_l^*} = V_l\angle 0$. The voltage injected by the UPQC series converter is expressed as $\mathbf{V_{f_1}} = V_{f_1}\angle\phi_{f_1}$. By incorporating these in (12) can be rewritten as follows:

$$\begin{aligned} \mathbf{V_{f_1}} &= \mathbf{V_l^*} - \mathbf{V_{t_1}} \\ V_{f_1}\angle\phi_{f_1} &= V_l\angle 0 - V_{t_1}\angle\delta_{t_1}. \end{aligned} \tag{13}$$

Solving (13) for voltage magnitude V_{f_1} and phase angle ϕ_{f_1} are given as follows:

$$V_{f_1} = \pm V_{t_1}\sqrt{K^2 + 1 - 2K\cos\delta_{t_1}} \tag{14}$$

and

$$\phi_{f_1} = \tan^{-1}\left(\frac{\sin\delta_{t_1}}{\cos\delta_{t_1} - K}\right) \tag{15}$$

where K is the ratio of V_l and V_{t_1}. The positive and negative values of V_{f1} indicate the reference during voltage sag and swell, respectively. δ_{t_1} is the phase angle of the fundamental positive sequence of grid terminal voltage.

The series converter also supplies the required harmonic component of voltage to compensate for the grid terminal voltage harmonics. Therefore, voltage injected (v_f^*) by UPQC series converter is given as follows:

$$v_f^* = v_{f_1} - v_{t_{\text{rest}}} \tag{16}$$

where $v_{t_{\text{rest}}}$ is the source terminal voltage harmonic component. Using (14)–(16), the UPQC series converter injected voltage ($v_{f_a}^*$, $v_{f_b}^*$, and $v_{f_c}^*$) references are given as follows:

$$\begin{aligned} v_{f_a}^* &= \sqrt{2}V_{f_1}\sin(\omega t + \phi_{f_1}) - v_{ta_{\text{rest}}} \\ v_{f_b}^* &= \sqrt{2}V_{f_1}\sin\left(\omega t + \phi_{f_1} - \frac{2\pi}{3}\right) - v_{tb_{\text{rest}}} \\ v_{f_c}^* &= \sqrt{2}V_{f_1}\sin\left(\omega t + \phi_{f_1} - \frac{4\pi}{3}\right) - v_{tc_{\text{rest}}}. \end{aligned} \tag{17}$$

These voltages are injected by UPQC series converter to maintain PCC voltage at nominal value. The hysteresis-based voltage controller is used to control the UPQC series converter. This controller compares the actual voltages of the UPQC series converter and its reference voltage using (17) to generate pulses for the UPQC series converter.

B. BESS DC–DC Converter

The BESS dc–dc converter is connected at the dc link of the UPQC converters. It supplies the power losses in the dc grid and exchanges active power during LVac voltage disturbances. The BESS dc–dc converter controls the dc link voltage of UPQC. During voltage sag, the BESS dc–dc converter supplies active power which is injected into LVac grid to maintain the LVac voltage. During the voltage swell, the UPQC needs to absorb the active power to maintain the PCC voltage. In this case, the BESS absorbs the active power.

Depending upon the power absorption or support from the BESS, the current direction of the BESS converter will change to maintain the dc link voltage of UPQC. It compares the actual dc link voltage (V_{dc}) with reference voltage (V_{dc}^*) and an error is generated. This error is passed through the proportional and integral (PI) controller to generate the switching pulses for the BESS dc–dc converter [24].

C. PV and EV DC—AC Converters

The dc—ac converters of PV and EV exchanges the required active power with ac and dc grids. The ith bus dc—ac

converter reference currents (i^*_{ca-i}, i^*_{cb-i}, and i^*_{cc-i}) to share active power are given as follows:

$$i^*_{ca-i} = \frac{v^+_{la1-i}}{\left(v^+_{la1-i}\right)^2 + \left(v^+_{lb1-i}\right)^2 + \left(v^+_{lc1-i}\right)^2} P^*_{C-i}$$
$$i^*_{cb-i} = \frac{v^+_{lb1-i}}{\left(v^+_{la1-i}\right)^2 + \left(v^+_{lb1-i}\right)^2 + \left(v^+_{lc1-i}\right)^2} P^*_{C-i}$$
$$i^*_{cc-i} = \frac{v^+_{lc1-i}}{\left(v^+_{la1-i}\right)^2 + \left(v^+_{lb1-i}\right)^2 + \left(v^+_{lc1-i}\right)^2} P^*_{C-i} \quad (18)$$

where v^+_{la1-i}, v^+_{lb1-i}, and v^+_{lc1-i} are ith bus positive sequence component of voltages. P^*_{C-i} is the reference active power for ith bus of PV/EV dc—ac converter in each mode of operation. The hysteresis current controller generates pulses for PV/EV dc—ac converter to maintain the reference current of respective converters.

V. Loading Capacity of Distribution System

The loading capacity of the distribution system is limited by the voltage variations due to the loading at various buses [6]. The loads such as EV charging stations add extra loading on the existing distribution systems. This section investigates the impact of the EV charging stations penetration on a conventional LVac distribution system and compares performance with the proposed meshed hybrid microgrid system. A conventional LVac distribution system is shown in Fig. 4, the voltage at ith bus ($\mathbf{V_{l-i}}$) is given by

$$\begin{aligned}\mathbf{V_{l-i}} = \mathbf{V_l} &- (\mathbf{I_{ln}} + \mathbf{I_{ln-1}} + \cdots + \mathbf{I_{l1}})\mathbf{Z_l} m_n \\ &- (\mathbf{I_{ln-1}} + \mathbf{I_{ln-2}} + \cdots + \mathbf{I_{l1}})\mathbf{Z_l} m_{n-1} \\ &- \cdots - (\mathbf{I_{li}} + \mathbf{I_{li-1}} + \cdots + \mathbf{I_{l1}})\mathbf{Z_l} m_i \end{aligned} \quad (19)$$

where $\mathbf{V_l}$ is the voltage at PCC and i varies from 1 to n. $\mathbf{I_{ln}}, \mathbf{I_{ln-1}}, \ldots, \mathbf{I_{l1}}$ are load currents at respective buses. $\mathbf{Z_l}$ is the per-kilometer impedance and $m_n, m_{n-1}, \ldots, m_i$ are the lengths of each sections of the LVac line.

The voltage at ith bus is assumed as $\mathbf{V_{l-i}} = V_{l-i}\angle\delta_i$ and at PCC is $\mathbf{V_l} = V_l\angle 0$. For analyzing the voltage drops, the loading on each bus is considered uniform without any generation. In addition, a constant current absorption is considered at each bus [25]. Therefore, $\mathbf{I_{ln}} = \mathbf{I_{ln-1}} = \cdots = \mathbf{I_{l1}} = I_l\angle\phi_l$, where ϕ_l is the power factor angle. For the LVac grid, the R/X ratio is considered high [26]; therefore, $\mathbf{Z_l} \approx R_l$. Considering the equal spacing between buses, $m_n = m_{n-1} = \cdots = m_1 = m_l$. Hence, (19) is rewritten as follows:

$$\mathbf{V_{l-i}} = \mathbf{V_l} - nR_l m_l \mathbf{I_l} - (n-1)R_l m_l \mathbf{I_l} - \cdots - iR_l m_l \mathbf{I_l}. \quad (20)$$

Further simplification of (20) leads to

$$\mathbf{V_{l-i}} = \mathbf{V_l} - K_b K_{rl} \mathbf{I_l}$$
$$V_{l-i}\angle\delta_i = V_l - K_b K_{rl} I_l \angle\phi_l. \quad (21)$$

Solving (21) gives V_{l-i} as

$$V_{l-i} = \sqrt{V_l^2 + K_b^2 K_{rl}^2 I_l^2 - 2V_l K_b K_{rl} I \cos\phi_l}. \quad (22)$$

Based on the loading, the voltage magnitude at each bus changes. This leads to maximum voltage variations at the end buses. A case study is considered for the voltage variation in a multiple-bus LVac distribution system.

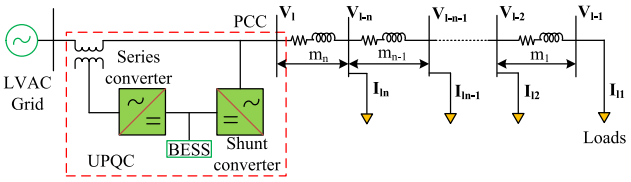

Fig. 4. Power flow paths in a conventional distribution system.

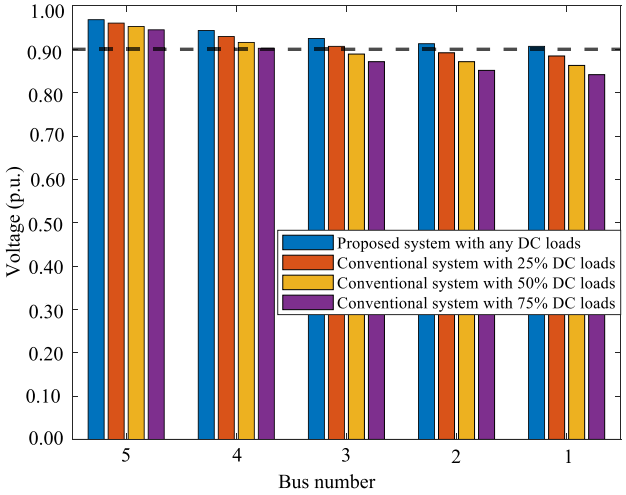

Fig. 5. Bus voltage variations in conventional [20] and the proposed systems.

A. Case Study

In this study, a five-bus LVac distribution system is considered. For per unit (p.u.) calculation, the base voltage is considered as 0.4 kV and the base power is considered as 100 kV·A. The nominal currents at each bus are considered as 0.08 p.u., which leads to a minimum permissible voltage (0.9 p.u.) at the farthest bus from PCC [27]. For the experiment, extra dc loads are added to the LVac grid at 25%, 50%, and 75% of the nominal LVac loads in three different cases. The voltages at each bus are plotted under respective conditions in Fig. 5. For the proposed system, the dc loads are added to the dc grid. The active power to the dc loads is supplied through the active power exchange capability of the UPQC shunt converter. Therefore, the voltages of ac grid buses are maintained within the permissible limits after the addition of dc loads.

Fig. 5 shows that when the loads are increased at each bus by 25%, 50%, and 75%, the voltage at bus 1–bus 3 are violated in the conventional system. Moreover, with the proposed system voltage at buses is maintained within grid code limits. This shows that in distribution grids where the R/X ratio is high, active power exchange has a greater impact on voltage compared to reactive power. The additional extra loads draw more active power from the grid through the LVac line which leads to under voltage at far-end buses in the conventional system. This analysis shows that the proposed distribution system where the high R/X ratio be utilized to integrate additional dc loads such as EV charging stations to the existing distribution system without violating the voltage limits. The performance comparison is given in Table I. For showing the benefits of the proposed system, its performance is compared with respect to the conventional system against various parameters.

TABLE I
PERFORMANCE COMPARISON

Parameter	Conventional System	Proposed System
Utilization of DG converter rating (kVA)	Limited utilization as the DG converter operation depends upon the PV power availability in [20], [28].	Various power flow paths allow higher utilization of DG converter.
LVAC line loss	Higher line losses due to flow of both active and reactive powers in LVAC line [20], [28].	Active power is possible through LVDC line and DG converter leading to lower LVAC line losses.
Continuous power supply during DG faults or service	Not possible [14], [20], [28]	Possible
Increase loading capacity	Not possible [20], [28]	Possible
Centralized control of reactive power	Moderate [10], [14], [20]	Higher as compared to conventional system.

TABLE II
SIMULATION PARAMETERS

System Quantities	Values
LVAC grid voltage	400 V (L-L)
LVDC grid voltage	1.2 kV
UPQC series converter	Transformer ratio = 1 : 1, S_{rse}= 50 kVA, L_f = 3 mH, C_f = 20 μF, R_d = 40 Ω
UPQC shunt converter	S_{rsh} = 50 kVA, L_{s1} = 2 mH, C_s = 20 μF, R_s = 40 Ω, L_{s2} = 1 mH
PV DC-AC converter	S_{rPV} = 50 kVA, C_{DC1} = 2200 μF, L_{fm1} = 6 mH, L'_{fm1} = 68μH, C_{fm1} = 10 μF, R_{d1} = 1 Ω
EV DC-AC converter	S_{rEV} = 25 kVA, C_{DC2} = 2200 μF, L_{fm2} = 4 mH, L'_{fm2} = 45 μH, C_{fm2} = 15 μF, R_{d2} = 1 Ω

VI. SIMULATION RESULTS

The meshed hybrid microgrid configuration with UPQC having two-bus is used for the simulation studies. The EV load and the PV source are connected to bus 1 and bus 2, respectively. In addition, dc and ac loads are considered on LVdc line and LVac line, respectively. For simulation studies, three cases are considered and system parameters are given in Table II. The simulation parameters for UPQC are based on [29]. The DG converter parameters are selected based [30], and PV and BESS are designed based on [14].

The BESS model uses a bidirectional dc–dc converter to increase the battery voltage to connect the common dc link voltage of the UPQC. The BESS maintained the dc link voltage of UPQC and supply power losses in LVdc line. However, BESS exchanges active power with the LVdc grid to ensure a stiff dc link voltage.

For three-phase, four-wire dc—ac converter, the minimum dc voltage across each capacitor should be 1.6–2.0 times the peak ac side phase voltage to ensure satisfactory performance [31]. In LVdc distribution grid, IEC 60 038 standards have set the limit for maximum LVdc voltage as 1500 V [32]. In this article, the LVac voltage is 400 V (L–L) for simulation studies. Therefore, the total LVdc voltage is set at 1.2 kV (600 V across each capacitor).

In [32] and [33], a comprehensive analysis of the protection and safety features in LVdc distribution grids is discussed. Protective devices, such as fuses, dc contactors, and circuit breakers, provide the necessary protection against overcurrent and short circuits, ensuring reliable and safe operation. Moreover, the use of hybrid circuit breakers has been suggested in the literature which integrates a mechanical breaker along with a power electronic switch.

A. Grid Voltage Sag Operation

Fig. 6 shows the operation of the system during a symmetrical grid voltage sag. The power sharing by EV and PV dc—ac converter is based on their rating. Fig. 6(a) shows the grid voltage waveform, where a symmetrical voltage sag is created. The LVac PCC voltages are maintained at nominal value by UPQC series converter, as shown in Fig. 6(b). Fig. 6(c) shows the voltage injected by the UPQC series converter. The LVac load and grid currents are shown in Fig. 6(d) and (e), respectively. The grid currents are balanced and sinusoidal irrespective of LVac load nature. The UPQC series and shunt converters power are shown in Fig. 6(f). The reactive and harmonic powers are provided by the UPQC shunt converter, and the active power supply by it is 0. The PV and EV dc—ac converter supply active power to the grid based on their rating and LVdc load power is shown in Fig. 6(g). The LVac grid power is low during the grid voltage sag, and LVac load power is shown in Fig. 6(h). During grid voltage sag, active power absorbed from dc link as the LVac loads are at a fixed value.

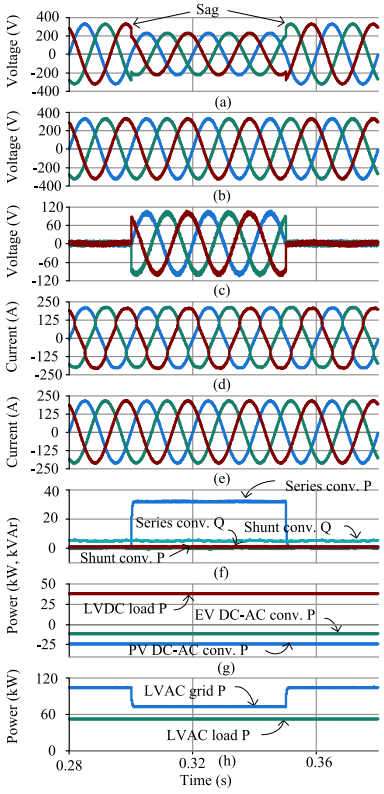

Fig. 6. Simulation results for grid voltage sag operation. (a) Grid voltages. (b) Voltage at PCC. (c) UPQC series converter voltage. (d) LVac load currents at PCC. (e) Grid currents. (f) UPQC series and shunt converter powers. (g) LVdc load and dc—ac converter powers. (h) LVac grid and load powers.

B. Operation During High DC Loads

Fig. 7 shows high-dc load operation of a meshed hybrid microgrid with UPQC. The high loading in LVdc grid and

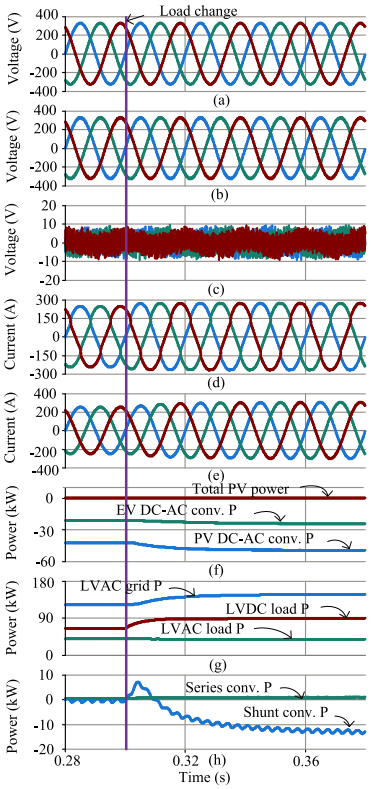

Fig. 7. Simulation results for high dc load operation. (a) Grid voltages. (b) Voltage at PCC. (c) UPQC series converter voltages. (d) LVac load currents at PCC. (e) Grid currents. (f) PV generation, EV, and PV dc—ac converter powers. (g) Grid, LVac, and LVdc powers. (h) UPQC shunt and series converter powers.

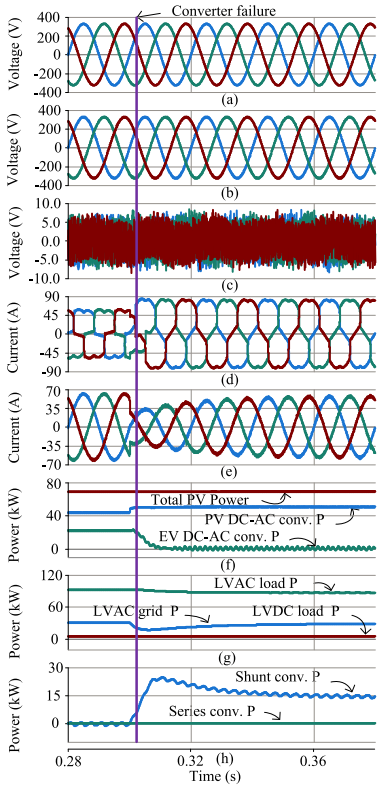

Fig. 8. Simulation results for EV dc—ac converter failure operation. (a) Grid voltages. (b) PCC voltages. (c) UPQC series converter voltage. (d) LVac load currents at PCC. (e) Grid currents. (f) PV generation, EV, and PV dc—ac converter powers. (g) Grid, LVac, and LVdc powers. (h) UPQC shunt and series converter powers.

also, the EV and PV dc—ac converters are unable to support the total active power requirement of the LVdc grid. The remaining active power is supplied from the UPQC shunt converter. The high dc loads lead to drawing non-sinusoidal current from the LVac grid. The LVac currents are the currents drawn by the LVac loads. The presence of non-linear loads in the LVac network results in nonsinusoidal currents being drawn. Therefore, these currents are not purely sinusoidal. The UPQC shunt converter supplies the reactive, and harmonic components of LVac loads so that the grid supplies balance and sinusoidal currents. Fig. 7(a) shows the grid voltage waveforms under normal operating conditions. The nominal voltage is maintained at LVac PCC as shown in Fig. 7(b). The voltages injected by the UPQC series converter are shown in Fig. 7(c). The LVac load currents and grid currents are shown in Fig. 7(d) and (e), respectively. When the high dc load occurs, EV and PV dc—ac converter works as per their maximum power rating, as shown in Fig. 7(f), and the UPQC shunt converter draws the balance power from the grid, as shown in Fig. 7(h).

C. Operation During EV DC—AC Converter Failure

In this mode, the PV power generation is at a high level and low-dc loading at the LVdc line. When the EV dc—ac converter fails, the power from dc grid is routed to ac grid via UPQC shunt converter. In Fig. 8(a), per phase grid voltage waveform are shown. The UPQC series converter maintains PCC voltage at the desired level as shown in Fig. 8(b). The injected voltage of the UPQC series converter is shown in Fig. 8(c). The grid current and LVac load currents are shown in Fig. 8(d) and (e), respectively. The active power flow from UPQC shunt converter during EV dc—ac converter fails is shown in Fig. 8(h). The LVac load and grid power are shown in Fig. 8(g). The PV generation, PV dc—ac, and EV dc—ac converters power are shown in Fig. 8(f).

VII. Experimental Studies

A prototype of the UPQC-based meshed hybrid system is developed in the laboratory. The block diagram of the prototype of the experimental setup is shown in Fig. 9. The experimental setup consists of UPQC, BESS, and DG converter. The UPQC has two dc—ac converters connected in series and shunt with LVac grids. The series dc—ac converter is connected with the LVac grid using an isolation transformer. The shunt dc—ac converter is connected to the LVac load side. The DG dc—ac converter is connected at bus 1, as shown in Fig. 9(a). The BESS converter is connected to the common dc link of UPQC converters. Bus 1 is formed by connecting resistance R_1 and inductance L_1. R_{dc_1} is the LVdc line resistance connecting between the dc link of UPQC and dc link of the DG converter.

The experiments are conducted at the scaled-down voltage and load. However, the nature of the connected loads and sources are similar to the simulated grid scenarios. This allows us to obtain experimental results similar to simulation results for various load conditions such as grid voltage sag/swell, power routing during high PV generation and/or peak EV loading, and DG failure condition.

The LVac grid voltage is selected as 110 V (L–L). The dc link voltage of UPQC is maintained at 310 V by BESS.

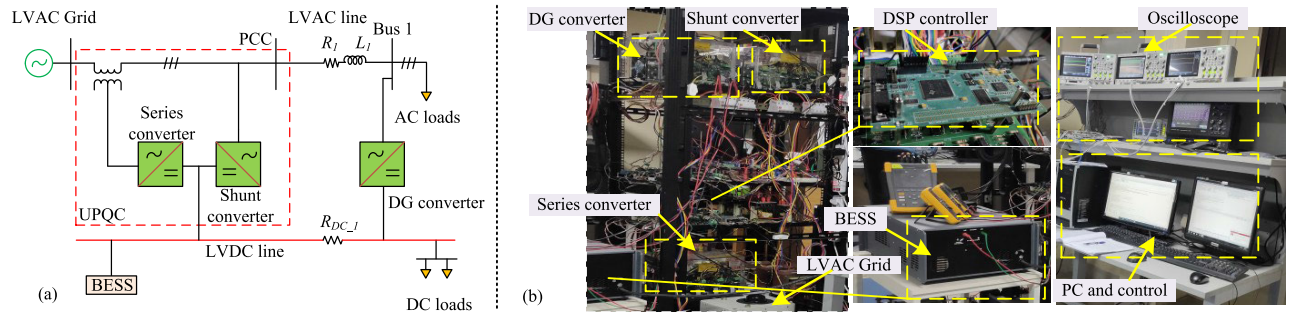

Fig. 9. Experimental setup. (a) Circuit connection. (b) Photograph of the hardware prototype.

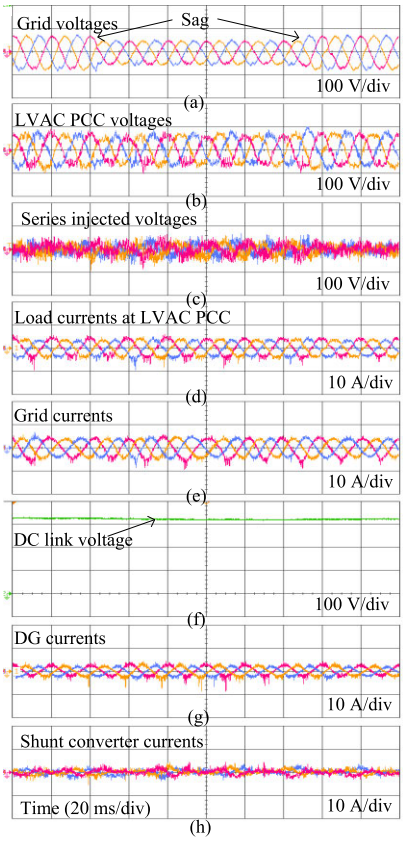

Fig. 10. Experimental results for grid voltage sag operation. (a) Grid voltages. (b) PCC voltages. (c) UPQC series converter voltages. (d) LVac load currents. (e) Grid currents. (f) DC link voltage. (g) DG currents. (h) UPQC shunt converter currents.

Fig. 9(b) shows the picture of the hardware prototype. All three cases shown in simulations are exhibited in experimental analysis.

A. Grid Voltage Sag Operation

Fig. 10 exhibits the results for the grid voltage sag condition. In Fig. 10(a), symmetrical grid voltage sag occurs as seen in the waveform. The nominal voltage of 110 V is maintained at PCC, as shown in Fig. 10(b). The series injected voltage during the sag period is shown in Fig. 10(c). Fig. 10(d)–(h), respectively, shows the load currents, source currents, dc link voltage, DG currents, and shunt converter currents during the operation. It is observed that the grid current is always sinusoidal irrespective of the nature of LVac loads, which is maintained by UPQC shunt converter. The load terminal voltage is maintained constant during grid voltage disturbances

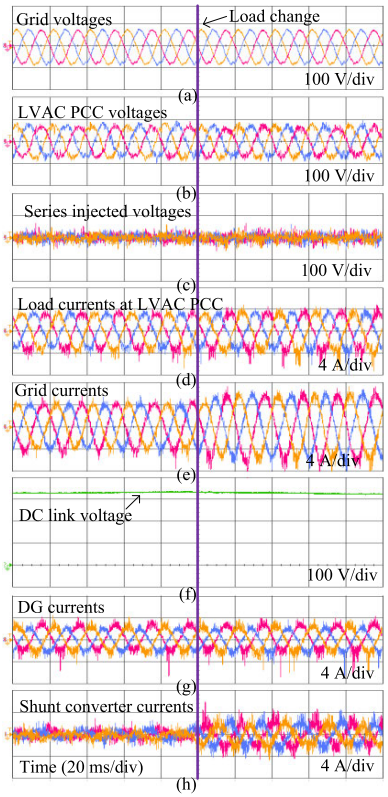

Fig. 11. Experimental results for high-dc load operation. (a) Grid voltages. (b) PCC voltages. (c) UPQC series converter voltages. (d) LVac load currents. (e) Grid currents. (f) DC link voltage. (g) DG currents. (h) UPQC shunt converter currents.

by the series converter. The DG converter transfers balanced power between the LVdc and LVac buses.

B. Operation During High DC Loads

In Fig. 11, the load change scenario is exhibited. The grid voltages, PCC voltages, UPQC series converter injected voltages, load currents, grid currents, and the dc link voltage are shown in the Fig. 11(a)–(f), respectively. The load change is marked in the waveforms. The DG currents reach the maximum rating as shown in Fig. 11(g). The extra dc load is absorbed through the UPQC shunt converter as seen in Fig. 11(h). The slight increment in the source current can be noted at this point, as shown in Fig. 11(e).

C. Operation During DG DC—AC Converter Failure

Fig. 12 shows the experimental results when the DG converter fails. The grid voltages and PCC voltages are

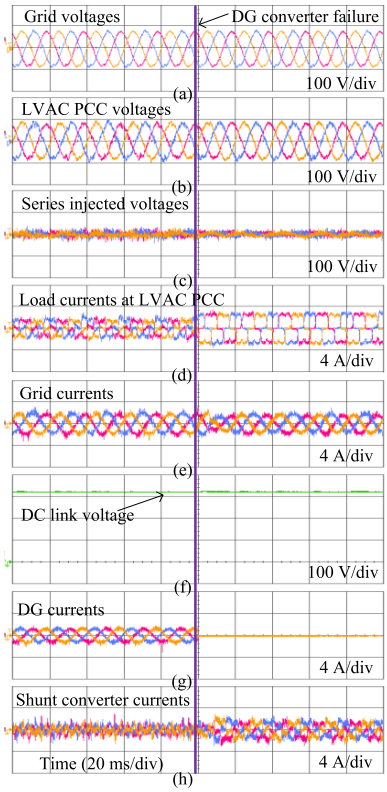

Fig. 12. Experimental results during DG converter failure condition. (a) Grid voltages. (b) PCC voltages. (c) UPQC series converter voltages. (d) LVac load currents. (e) Grid currents. (f) DC link voltage. (g) DG currents. (h) UPQC shunt converter currents.

maintained at the nominal value as shown in Fig. 12(a) and (b), respectively. The series injected voltages are shown in Fig. 12(c). During the fault condition or maintenance, the DG converter is disconnected from operation. In this case, the power exchanged by the DG converter becomes zero. However, the remaining DG and UPQC shunt converters must share the load power requirement. This results in more current flowthrough these converters. The load power shared by the faulty DG converter is provided through the UPQC shunt converter. As shown in Fig. 12(d) the LVac load current increases. The grid currents and dc link voltage are shown in Fig. 12(e) and (f), respectively. The DG dc—ac converter is disconnected after failure as shown in Fig. 12(g). At this point, the faulty DG converter's power from the dc grid is supplied via UPQC shunt converter, as shown in Fig. 12(h). The UPQC shunt converter currents are increased while the grid current remains unchanged.

VIII. Conclusion

The operation of a UPQC-based meshed hybrid microgrid is analyzed in this article. The meshed hybrid microgrid system improves the load and generation hosting capacity of a conventional distribution network by improving the voltage profile of the LVac load buses. The system also provides a better reliability during PV/EV dc—ac converter failure by routing power between LVac and LVdc lines. The power supply is distributed over multiple dc—ac converters. In addition, the UPQC provides the voltage and current quality conditioning services to the distribution grid. The simulation and experimental results show the performance of the proposed system under various operating conditions.

References

[1] X. Liang, "Emerging power quality challenges due to integration of renewable energy sources," *IEEE Trans. Ind. Appl.*, vol. 53, no. 2, pp. 855–866, Mar. 2017.

[2] A. Gupta, S. Doolla, and K. Chatterjee, "Hybrid AC–DC microgrid: Systematic evaluation of control strategies," *IEEE Trans. Smart Grid*, vol. 9, no. 4, pp. 3830–3843, Jul. 2018.

[3] S. Alshahrani, M. Khalid, and M. Almuhaini, "Electric vehicles beyond energy storage and modern power networks: Challenges and applications," *IEEE Access*, vol. 7, pp. 99031–99064, 2019.

[4] T. V. Thang, A. Ahmed, C.-I. Kim, and J.-H. Park, "Flexible system architecture of stand-alone PV power generation with energy storage device," *IEEE Trans. Energy Convers.*, vol. 30, no. 4, pp. 1386–1396, Dec. 2015.

[5] J. von Appen, M. Braun, T. Stetz, K. Diwold, and D. Geibel, "Time in the sun: The challenge of high PV penetration in the German electric grid," *IEEE Power Energy Mag.*, vol. 11, no. 2, pp. 55–64, Mar. 2013.

[6] S. K. Chaudhary, J. M. Guerrero, and R. Teodorescu, "Enhancing the capacity of the AC distribution system using DC interlinks—A step toward future DC grid," *IEEE Trans. Smart Grid*, vol. 6, no. 4, pp. 1722–1729, Jul. 2015.

[7] Y. Liu, H. Li, X. Zhang, G. Feng, and Z. Du, "V2G integration based on a UPQC with SMES," *IEEE Trans. Appl. Supercond.*, vol. 34, no. 8, pp. 1–3, Nov. 2024.

[8] D. I. Brandao, R. P. D. Santos, W. W. A. G. Silva, T. R. Oliveira, and P. F. Donoso-Garcia, "Model-free energy management system for hybrid alternating current/direct current microgrids," *IEEE Trans. Ind. Electron.*, vol. 68, no. 5, pp. 3982–3991, May 2021.

[9] R. Zhu, M. Liserre, M. Langwasser, and C. Kumar, "Operation and control of the smart transformer in meshed and hybrid grids: Choosing the appropriate smart transformer control and operation scheme," *IEEE Ind. Electron. Mag.*, vol. 15, no. 1, pp. 43–57, Mar. 2021.

[10] R. R. A. Núñez, J. Posada, C. Unsihuay-Vila, and O. Pinzón-Ardila, "Review of smart transformer-based meshed hybrid microgrids: Shaping, topology and energy management systems," *IEEE Access*, vol. 11, pp. 130165–130185, 2023.

[11] V. Jain and B. Singh, "Power quality improvement in PV system tied to weak grid," *IEEE Trans. Ind. Appl.*, vol. 57, no. 2, pp. 1265–1273, Mar. 2021.

[12] P. Shukl and B. Singh, "Recursive digital filter based control for power quality improvement of grid tied solar PV system," *IEEE Trans. Ind. Appl.*, vol. 56, no. 4, pp. 3412–3421, Jul. 2020.

[13] S. K. Dash and P. K. Ray, "A new PV-open-UPQC configuration for voltage sensitive loads utilizing novel adaptive controllers," *IEEE Trans. Ind. Informat.*, vol. 17, no. 1, pp. 421–429, Jan. 2021.

[14] M. A. Mansor, K. Hasan, M. M. Othman, S. Z. B. M. Noor, and I. Musirin, "Construction and performance investigation of three-phase solar PV and battery energy storage system integrated UPQC," *IEEE Access*, vol. 8, pp. 103511–103538, 2020.

[15] C. Kumar, M. K. Mishra, and S. Mekhilef, "A new voltage control strategy to improve performance of DSTATCOM in electric grid," *CES Trans. Electr. Mach. Syst.*, vol. 4, no. 4, pp. 295–302, Dec. 2020.

[16] C. Kumar and M. K. Mishra, "Predictive voltage control of transformer-less dynamic voltage restorer," *IEEE Trans. Ind. Electron.*, vol. 62, no. 5, pp. 2693–2697, May 2015.

[17] S. Devassy and B. Singh, "Design and performance analysis of three-phase solar PV integrated UPQC," *IEEE Trans. Ind. Appl.*, vol. 54, no. 1, pp. 73–81, Jan. 2018.

[18] P. Ray, P. K. Ray, and S. K. Dash, "Power quality enhancement and power flow analysis of a PV integrated UPQC system in a distribution network," *IEEE Trans. Ind. Appl.*, vol. 58, no. 1, pp. 201–211, Jan. 2022.

[19] C. D. Sanjenbam, B. Singh, and P. Shah, "Reduced voltage sensors based UPQC tied solar PV system enabling power quality improvement," *IEEE Trans. Energy Convers.*, vol. 38, no. 1, pp. 392–403, Mar. 2023.

[20] S. Devassy and B. Singh, "Performance analysis of solar PV array and battery integrated unified power quality conditioner for microgrid systems," *IEEE Trans. Ind. Electron.*, vol. 68, no. 5, pp. 4027–4035, May 2021.

[21] V. M. Hrishikesan, D. Kumar, D. Das, and C. Kumar, "Operation and control of unified power quality conditioner enabled meshed hybrid microgrid," in *Proc. IEEE 15th Int. Conf. Compat., Power Electron. Power Eng. (CPE-POWERENG)*, Jul. 2021, pp. 1–6.

[22] A. Ghosh and G. Ledwich, *Power Quality Enhancement Using Custom Power Devices*. Cham, Switzerland: Springer, 2012.

[23] A. Ghosh and G. Ledwich, "Compensation of distribution system voltage using DVR," *IEEE Trans. Power Del.*, vol. 17, no. 4, pp. 1030–1036, Oct. 2002.
[24] S. Pala and S. P. Singh, "Design, modeling and implementation of bi-directional buck and boost converter," in *Proc. IEEE 5th India Int. Conf. Power Electron. (IICPE)*, Dec. 2012, pp. 1–6.
[25] D. Das, V. M. Hrishikesan, C. Kumar, and M. Liserre, "Smart transformer-enabled meshed hybrid distribution grid," *IEEE Trans. Ind. Electron.*, vol. 68, no. 1, pp. 282–292, Jan. 2021.
[26] J. Rocabert, A. Luna, F. Blaabjerg, and P. Rodríguez, "Control of power converters in AC microgrids," *IEEE Trans. Power Electron.*, vol. 27, no. 11, pp. 4734–4749, Nov. 2012.
[27] H. Markiewicz and A. Klajn, "Standard EN 50160-voltage characteristics in public distribution systems," Wroclaw, Poland, Wroclaw Univ. Technol., Tech. Rep. Jul. 2004.
[28] S. K. Yadav, A. Patel, and H. D. Mathur, "Study on comparison of power losses between UPQC and UPQC-DG," *IEEE Trans. Ind. Appl.*, vol. 58, no. 6, pp. 7384–7395, Nov. 2022.
[29] C. Kumar, M. K. Mishra, and M. Liserre, "LCL filter based UPQC configuration for power quality improvement," in *Proc. IEEE Power Energy Soc. Gen. Meeting (PESGM)*, Jul. 2016, pp. 1–5.
[30] M. Liserre, F. Blaabjerg, and S. Hansen, "Design and control of an LCL-filter-based three-phase active rectifier," *IEEE Trans. Ind. Appl.*, vol. 41, no. 5, pp. 1281–1291, Oct. 2005.
[31] M. K. Mishra and K. Karthikeyan, "An investigation on design and switching dynamics of a voltage source inverter to compensate unbalanced and nonlinear loads," *IEEE Trans. Ind. Electron.*, vol. 56, no. 8, pp. 2802–2810, Aug. 2009.
[32] E. Rodriguez-Diaz, F. Chen, J. C. Vasquez, J. M. Guerrero, R. Burgos, and D. Boroyevich, "Voltage-level selection of future two-level LVdc distribution grids: A compromise between grid compatibiliy, safety, and efficiency," *IEEE Electrific. Mag.*, vol. 4, no. 2, pp. 20–28, Jun. 2016.
[33] R. Lazzari and L. Piegari, "Design and implementation of LVDC hybrid circuit breaker," *IEEE Trans. Power Electron.*, vol. 34, no. 8, pp. 7369–7380, Aug. 2019.

Devendra Kumar (Student Member, IEEE) received the B.Tech. degree in electrical engineering from the National Institute of Technology Patna, Patna, India, in 2015, and the M.Tech. degree in power electronics and drives from the Indian Institute of Technology Mandi, Suran, India, in 2019.

He is currently a Research Scholar with the Department of Electronics and Electrical Engineering, Indian Institute of Technology Guwahati, Guwahati, India.

V. M. Hrishikesan received the B.Tech. degree in electrical and electronics engineering from the Government Engineering College, Thrissur, India, in 2011, the M.Tech. degree in power systems from the National Institute of Technology Tiruchirappalli, Tiruchirappalli, India, in 2014, and the Ph.D. degree from the Indian Institute of Technology Guwahati, Guwahati, India, in 2021.

He was a Research Assistant with the Chair of Power Electronics, Kiel University, Kiel, Germany. He is currently working with Siemens Gamesa Renewable Energy, Kongens Lyngby, Denmark.

Anup Kumar Deka received the B.Tech. degree in electrical and electronics engineering from Assam Don Bosco University, Guwahati, India, in 2013, and the M.S.E.E degree in power and energy systems from the University of Houston, Houston, TX, USA, in 2023.

He is working as a Power Electronics Engineer with Wright Electric Inc., Malta, NY, USA, working on various power electronics converter topologies and controls.

Dwijasish Das (Member, IEEE) received the B.E. degree in electrical engineering from the Assam Engineering College, Guwahati, India, in 2011, the M.Tech. degree in power electronics from the National Institute of Technology Tiruchirappalli, Tiruchirappalli, India, in 2015, and the Ph.D. degree from the Indian Institute of Technology Guwahati, Guwahati, in 2023.

He is currently a Post-Doctoral Researcher with the Department of Electrical Sustainable Energy, Delft University of Technology (TU Delft), Delft, The Netherlands.

Chandan Kumar (Senior Member, IEEE) received the B.Sc. degree in electrical engineering from the Muzaffarpur Institute of Technology, Muzaffarpur, India, in 2009, the M.Tech. degree in electrical engineering from the National Institute of Technology Tiruchirappalli, Tiruchirappalli, India, in 2011, and the Ph.D. degree in electrical engineering from the Indian Institute of Technology Madras, Chennai, India, in 2014.

He is currently working as an Associate Professor with the Electronics and Electrical Engineering Department, Indian Institute of Technology Guwahati, Guwahati, India.

Dr. Kumar is serving as an Associate Editor for IEEE SYSTEMS JOURNAL, IEEE OPEN JOURNAL OF POWER ELECTRONICS, IEEE OPEN JOURNAL OF THE INDUSTRIAL ELECTRONICS SOCIETY (OJIES), and IEEE ACCESS JOURNAL.

Mahesh K. Mishra (Senior Member, IEEE) received the B.Tech. degree in electrical engineering from the College of Technology, Pantnagar, India, in 1991, the M.E. degree in electrical engineering from the Indian Institute of Technology Roorkee, Roorkee, India, in 1993, and the Ph.D. degree in electrical engineering from the Indian Institute of Technology Kanpur, Kanpur, India, in 2002.

He has about 30 years of teaching and research experience. He was with the Department of Electrical Engineering, Visvesvaraya National Institute of Technology, Nagpur, India, for about ten years. He is currently a Professor with the Department of Electrical Engineering, Indian Institute of Technology Madras, Chennai, India. He has authored the book: *Power Quality in Power Distribution Systems: Concepts and Applications* (CRC Press, 2023). His research interests include power distribution systems, power electronic applications in microgrids, and renewable energy systems.

Dr. Mishra is a Life Member of the Indian Society of Technical Education. He received the IETE Prof. Bimal Bose Award, in 2015, for his outstanding contributions to power electronics applications in power systems. In November 2017, he was elected as a fellow of the Indian National Academy of Engineering. He received the IEEE PES India Narain Hingorani Award for Excellence in Custom Power Devices, in 2024. He also serves as the IEEE Madras Chapter Chair.